Cell. Mol. Life Sci. (2009) 66:3161–3175
DOI 10.1007/s00018-009-0075-6

Cellular and Molecular Life Sciences

REVIEW

Plant aquaporin selectivity: where transport assays, computer simulations and physiology meet

Uwe Ludewig · Marek Dynowski

Received: 22 April 2009 / Revised: 8 June 2009 / Accepted: 10 June 2009 / Published online: 30 June 2009

Abstract Plants contain a large number of aquaporins with different selectivity. These channels generally conduct water, but some additionally conduct NH_3, CO_2 and/or H_2O_2. The experimental evidence and molecular basis for the transport of a given solute, the validation with molecular dynamics simulations and the physiological impact of the selectivity are reviewed here. The aromatic/arginine (ar/R) constriction is most important for solute selection, but the exact pore requirements for efficient conduction of small solutes remain difficult to predict. Yeast growth assays are valuable for screening substrate selectivity and are explicitly shown for hydrogen peroxide and methylamine, a transport analog of ammonia. Independent assays need to address the relevance of different substrates for each channel in its physiological context. This is emphasized by the fact that several plant NIP channels, which conduct several solutes, are specifically involved in the transport of metalloids, such as silicic acid, arsenite, or boric acid in planta.

Keywords Hydrogen peroxide · Reactive oxygen species · Aquaglyceroporin · Molecular dynamics · Gas channel · Methylamine

U. Ludewig (✉)
Applied Plant Sciences, Institute of Botany,
Darmstadt University of Technology, Schnittspahnstr. 10,
64287 Darmstadt, Germany
e-mail: ludewig@bio.tu-darmstadt.de;
uwe.ludewig@zmbp.uni-tuebingen.de

M. Dynowski
Center for Plant Molecular Biology, Plant Physiology,
Auf der Morgenstelle 1, 72076 Tübingen, Germany

Introduction

The membrane that surrounds the cell and cellular compartments not only separates life from death, but also provides a low-dielectric barrier for charged and polar molecules. Classical studies have provided a solid basis for the lipid permeability of water and all physiologically relevant solutes [1, 2]. In addition to the intrinsic passive bilayer permeability, water and small solute flux across membranes is facilitated by aquaporins in all organisms. Their importance for human physiology is underscored by the fact that their loss can result in diseases [3]. Similarly, reduced growth or viability is associated with the loss of aquaporins in plants under laboratory conditions, and the relevance of these channels for survival in native environments is only beginning to be understood. Several excellent recent reviews have covered the function of plant aquaporins and their associated physiology [4, 5] and the in planta effects of the genetic modulation of aquaporin expression [6]. The transport of unconventional substrates, mostly by microbial and mammalian aquaporins, has also been summarized [7].

In this review, we will give an update on aquaporin selectivity with a focus on plant proteins. In order to understand their potential physiological function, we will discuss experimental findings and compare them with molecular dynamics (MD) computer simulations. Although we will discuss the permeation of small solutes, such as NH_3, CO_2 and O_2, we will not use the term "gas channel" in this context. This term may be misleading, as it implies that the surrounding waters have no impact on the diffusion of solutes. However, water–solute interactions and solute-induced water–protein interactions participate to determine channel selectivity. Furthermore, a "gas" defines a physical state of matter, but the volatile molecules referred to are

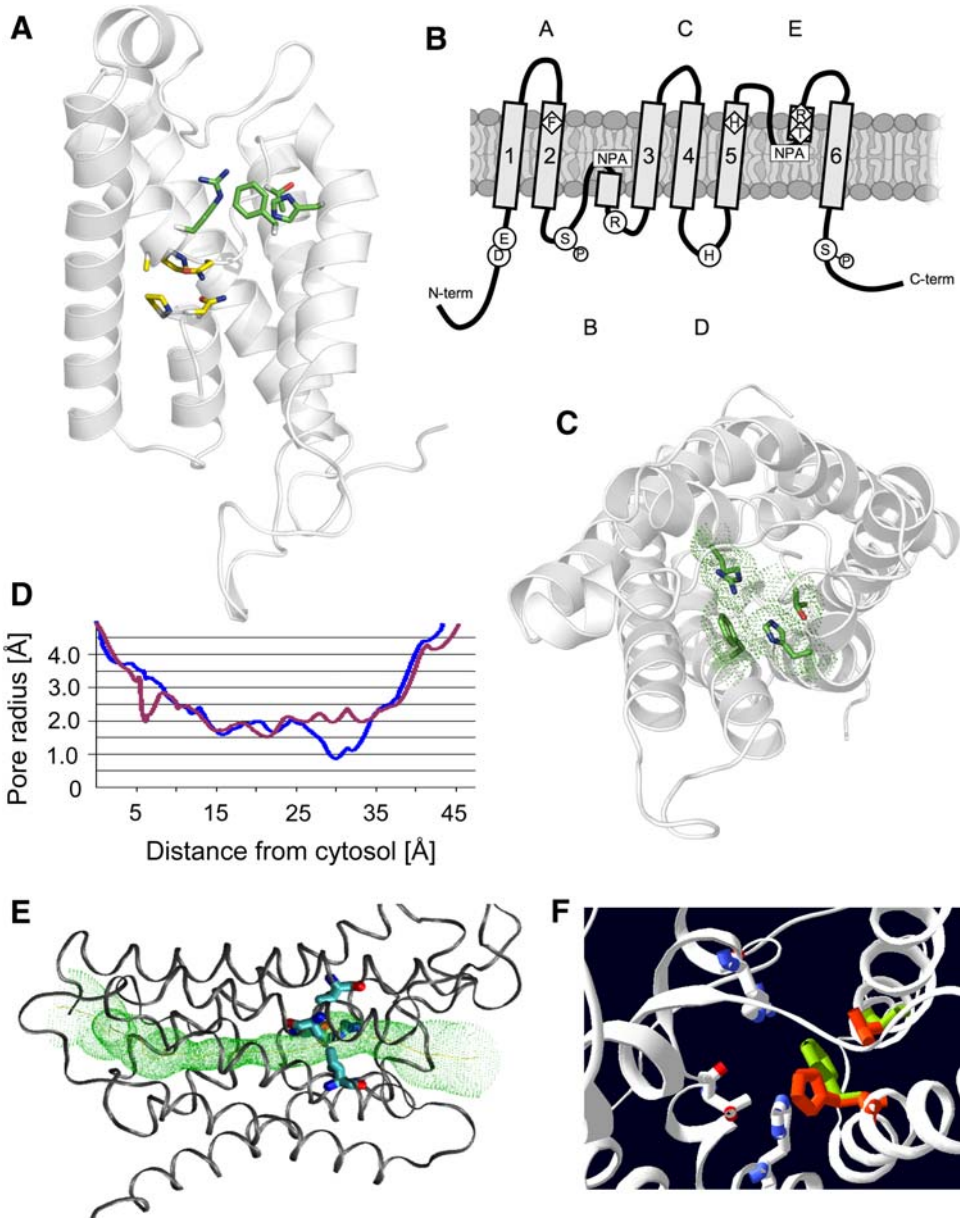

Fig. 1 Molecular structure of aquaporin monomers and the ar/R constriction. **a** Side view of the open *So*PIP2;1 pore in ribbon representation. Helices 1 and 2 were removed to open the view into the pore. The aromatic/arginine (ar/R) residues, F, H, T, and R are explicitly shown in *green*, the two NPA-stretches in *yellow*. **b** Schematic two-dimensional representation of the structure. Ar/R residues are shown in *diamonds*, whereas residues involved in gating are shown in *circles*. **c** Top view: the four residues of the constriction site (ar/R) are shown with their van der Waals radii. **d** Pore radius of *So*PIP2;1 (*blue*) and a mutant that has the ar/R filter as NIP5;1 (*violet*) calculated using the program HOLE. The structures were derived from the closed pore (PDB accession number 1Z98), in which Phe180–Leu200 was replaced by the open structure (2B5F). **e** Monomer of the NIP5;1-like mutant with pore calculated by hole as *green* mesh. **f** Residues in the constriction of *So*PIP2;1 with TIP-like ar/R constriction. A histidine residue that replaces the phenylalanine bends into the pore (*red*), as long as no compensatory mutation in an adjacent threonine (to glycine) is made (*green*)

dissolved in liquid water, and occur as gases only in their pure form under ambient conditions.

Plant aquaporin structure

Plants, such as rice, maize, and the model plant *Arabidopsis*, encode 31–39 aquaporin family members in the genome [8], while humans have 13. More than ten different high-resolution structures of aquaporin homologs have been determined, including an open and a closed structure of *So*PIP2;1 from spinach [9]. All structures show an extraordinary conservation in their overall transmembrane architecture, but differ in the loops exposed to the aqueous solutions. Each monomer forms a hydrophobic pore and aggregates to tetramers. A monomer is composed of six tilted, membrane-spanning helices that are connected by five loops (A–E) (Fig. 1a–c). In two of these loops (B and E), short helices dip back into the membrane from opposite sides and contain two NPA (Asn-Pro-Ala) motifs that are conserved in most aquaporins and meet at the center of the membrane. The aromatic/arginine (ar/R) region is located ~7 Å from the center towards the external pore vestibule, and is formed by residues from TM2, TM5 and two residues from loop E. These residues define the most constricted site of the channel, which is ~2 Å in diameter in the most water-selective aquaporins, such as *So*PIP2;1 (Fig. 1d). The pore diameter is ~1 Å larger in glycerol-conducting aquaporins (also termed aquaglyceroporins), such as the *E. coli* glycerol uptake facilitator GlpF. With

only a single exception, mammalian AQP6 that also transports anions, all family members exclusively facilitate the passive flow of small, uncharged solutes and/or water across membranes. Although the term aquaporin was originally used exclusively for the water-selective channels of the family, we will follow the now common nomenclature that adopted this term for all family members.

Plant aquaporins are often categorized according to their phylogenetic relationship, which by coincidence groups the family members according to their subcellular localization. The PIP1s (five members in *Arabidopsis*) and the PIP2s (eight members) are very closely related by sequence and are plasma membrane intrinsic proteins. The TIPs are tonoplast intrinsic proteins (ten members), small basic SIPs are localized in the endoplasmic reticulum (three members) [10] and most NOD26-related NIPs are localized to the plasma membrane (nine members). When heterologously expressed, all the plant PIPs, TIPs, SIPs, and NIPs (except for *At*NIP6;1, [11]) that could be functionally expressed, were permeable to water.

Water conduction

Water has an exceptional importance for plants, and the transpiration from the leaves of a large tree can approach 200 l per day. Plants are exposed to rapidly changing hostile environments, where periods of drought can be eventually followed by rainfall, and water logging of roots may suddenly occur. Many plant species are particularly efficient in coping with changes in water supply, to keep their metabolism intact. This is reflected by the various and complex levels of aquaporin regulation, which have been reviewed in more detail elsewhere [4–6].

Initial studies observed that many PIP2 members strongly increased the water permeability in the plasma membrane of heterologous expression systems, such as oocytes, but many PIP1 members exhibited low or no transport activity. PIP1s from maize form heterotetramers with PIP2s in oocytes [12] and in planta [13] and require these interactions to traffic to the plasma membrane. In the absence of PIP2s, the PIP1 proteins remained trapped in intracellular compartments [13]. Genetic interactions between PIP1 and PIP2 members were also suggested by a study in *Arabidopsis*, where members of both PIP groups were separately silenced, but the effects were not additive [14]. In this work, a lower root hydraulic conductivity was observed with individually silenced PIP1 or PIP2 isoforms, and the same reduction was observed when both families were suppressed by antisense [14].

In several studies, the PIP expression of different species was genetically reduced. The osmotic water permeability or root hydraulic conductivity was consistently decreased, but only to a limited extent, probably due to some redundancy. Early research with transgenic tobacco plants overexpressing aquaporins indicated that plant growth was enhanced by additional channels. These studies identified that the native, rather low symplastic water transport, was limiting optimal growth even under favorable conditions [15]. The strong *At*PIP1;2 expression in tobacco was not beneficial under salt stress and was deleterious during drought stress [15].

In several species, the expression levels of PIPs have been documented, together with their transcriptional changes upon stress. In a few cases, these analyses additionally quantified the different protein levels and revealed a rather consistent down-regulation of PIPs in roots with salt [16], drought [17], or cold stress [18, 19]. As exceptions, *At*PIP1;4, *At*PIP2;5, and *At*PIP2;6, which were more abundant in leaves and/or flowers, were unchanged or more strongly expressed under drought [17]. Upon salt treatment, the transcripts and proteins of all the significantly expressed PIPs and TIPs decreased in a coordinated manner. PIPs and TIPs were subcellularly re-localized to internal membranes or to vacuolar invaginations [16]. All these treatments reduced the water permeability across the plasma membranes, confirming the primary involvement of PIPs in water homeostasis in planta.

Since high-resolution structures are not available for all (or all classes of) aquaporins, it is common practice that important residues are deduced from sequence alignments. Homology models are frequently viewed with some skepticism, since biologically important structural details are often found in disparate loops that vary between individual homologs. However, surprisingly accurate predictions on membrane protein structures have been revealed by homology modeling, especially in the catalytically important membrane regions [20]. This modeling gave initial insights into the minimal pore diameters of aquaporins from *Arabidopsis* [21], and later from other plants [8]. Based on the available structures from many species, a model of *So*PIP2;1 showed an excellent agreement with the X-ray structures in the transmembrane region ([8]; Dynowski, unpublished).

All PIPs from *Arabidopsis*, maize and rice have an identical narrow ar/R selectivity filter (Fig. 1; Table 1). Structural modeling identified that almost the same residues line the pore, which suggests that the overall pore selectivity of all PIPs is virtually identical, irrespective of whether they are PIP1s or PIP2s. Many studies confirmed the large water transport capacity of PIPs, but experimental evidence suggests that individual PIPs may additionally transport other solutes. For example, *Nt*AQP1, a PIP1 member, transported as much glycerol as the bacterial glycerol channel GlpF in oocytes [22]. This is quite surprising, as mutational evidence from other aquaporins,

Table 1 Pore residues in plant PIP, TIP, and NIP channels at the ar/R filter

Position	H2	H5	LE1	LE2	NH_3	H_2O_2	PIP mutant NH_3	PIP mutant H_2O_2
At, *Zm*, *Os*: PIP1, PIP2	F	H	T	R	−	+	−	+
At, *Zm*, *Os*: TIP1	H	I	A	V	+	++	−	−
Zm, *Os*: TIP2, *At*TIP2, 3, 4	H	I, M, V	A, G, S	R	+	+	−	+
*Zm*TIP4, 5, *Os*TIP4, 5	H, Q, T	S, T, V	A	R			−	+
*At*TIP5;1	N	V	G	C			−	+
Zm, Os: NIP1, *At* NIP1, 2, 3, 4	W	I, V	A	R	+	+	+	+
*Os*NIP3, *Zm*NIP3, *At*NIP5, 6, 7	A	I, V, A	G, A, P	R			±	+
*Zm*NIP2, *Os*NIP2	G	S	G	R				
*Os*NIP4;1	C	G	G	R				
*Pf*AQP	W	G	F	R	+			
*h*AQP1	F	H	C	R	±			
*h*AQP1 mut (Ref. [42])	F, A	H, A	C	V	+			
*h*AQP3	F	G	Y	R	+			
*h*AQP7	E	G	Y	R	+			
*h*AQP8	H	I	G	R	+			
*h*AQP9	G	A	C	R	+			

Aquaporins for which NH_3 and H_2O_2 permeability has been experimentally determined are indicated with plus. PIP mutant constructs: mutations were introduced into *At*PIP2;1 [52]. The selectivity filter was identical to TIPs and NIPs, but failed to confirm the proposed permeability of native channels. The amino acids are given in single letter code

H2 Helix 2, *H5* helix 5, *LE1* loop E1, *LE2* loop E2

molecular dynamics computer simulations, and the fact that glycerol transport was exclusively found with aquaporins that have a larger pore diameter, contradict the view that PIPs can efficiently transport glycerol [23–25].

Plant plasma membrane aquaporin gating is complex

The molecular mechanism how plant aquaporins switch between open and closed states has recently been identified in PIP2s. A conserved histidine in the second intracellular loop (D) plays a key role and is protonated upon a drop in the cytoplasmic pH [26]. This acidification leads to a conformational change of loop D, which contains several hydrophobic residues that fold into a cavity near the cytosolic entrance, to block water permeation in the closed state [9]. This closing involves only minor structural changes in the overall pore structure and is restricted to the cytoplasmic vestibule, where it also involves the binding of divalent cations such as Ca^{2+}, Mn^{2+} or Cd^{2+} [27]. In the closed conformation, a divalent cation is coordinated by charged residues from loop D, the N-terminus and the first cytoplasmic loop [9]. The inter-dependence of the open state on the pH, divalent cations and phosphorylation of two serine residues was supported by MD computer simulations [9]. Recent mutational analysis confirmed the importance of the histidine in loop D for intracellular, pH-dependent opening and (partial) closing in other PIP aquaporins, but showed that the gating mechanism appears to be more complex [27, 28]. The importance of phosphorylation on the pH-dependent modification of water permeability could not be confirmed by transport assays with PIP channels that were mutated in the two key serine residues [28]. NIP and TIP channels are also reversibly phosphorylated, but at different positions, and whether they are gated is less clear.

To obtain a stable open structure for computer simulations, phosphorylation was necessary [9]. A modified high-resolution pore of *So*PIP2;1 in which only loop D from the low-resolution open structure was incorporated into the high-resolution closed structure (at 2.1 Å) yielded a stable structure, but it was necessary to phosphorylate the protein at the known serines (Fig. 1b) to maintain the open status of the chimeric structure [29].

Molecular dynamics simulations on aquaporins

Molecular dynamics simulations have become standard methods to understand lipid and protein function at atomic resolution. As early as high-resolution structures of aquaporins became available, the mechanism of water conduction was studied by MD simulations [23, 30]. The setup for these simulations typically involved a box containing the whole tetramer, embedded in a simple membrane and surrounded with water (Fig. 2a). The

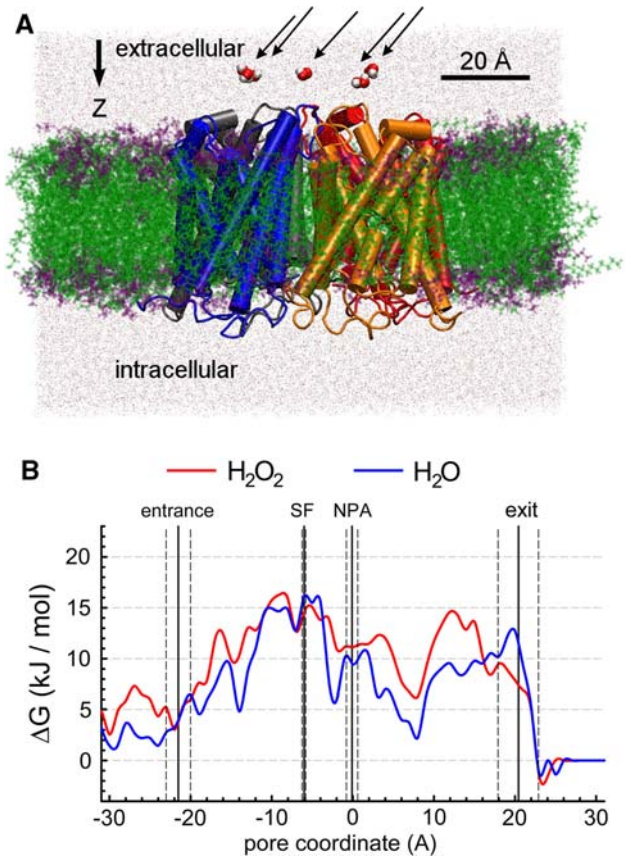

Fig. 2 Setup of MD simulations on tetrameric, open *So*PIP2;1 and energetic pore profile. **a** Side view of the tetramer embedded in a lipid bilayer with the individual starting positions of the five waters and H_2O_2 explicitly shown (*arrows*). Two monomers, in *blue* and *orange*, are seen in the foreground. **b** The energy profile deduced from the residence time for water (*blue*) and hydrogen peroxide (*red*) along the *So*PIP2;1 pore. The variance along the *z*-axis of the entrance, selectivity filter (SF, ar/R), NPA-region and exit on the cytosolic side is also shown. Modified after [29]

enormous increase in computer power and a better knowledge of the principles of membrane protein structure recently allowed the study of very detailed aspects of aquaporin function and yielded an atomic picture of the molecular mechanisms involved.

Molecular dynamics simulations describe the interactions of all atoms within a system using a relatively simple empirical potential function, a compromise between accuracy and computational efficiency. This potential function accounts for all the atomic interactions, such as stretching, bending, torsional interactions, van der Waals forces, and long-range electrostatic Coulomb interactions. From this potential function, the forces on all atoms in the system, often more than 100,000 atoms in total, are calculated and integrated in time, using time steps in the order of 10^{-15} s. This generates a trajectory that contains the diffusive movement of all lipids, proteins, waters, and other solutes, over millions of time steps. The further analysis can then provide insight into the fundamental mechanisms of the particular system and its thermodynamic properties.

Since 'real-time' MD simulations monitor rapid processes within a few ns at atomic resolution, spontaneous conduction attempts or full water permeation events in aquaporins were visualized and revealed molecular interaction energies and effects on the surrounding water [23, 30]. The simulations identified that the dynamic hydrogen bond interaction network in bulk water was efficiently replaced by equivalent hydrogen interactions donated by the pore. A favorable water-pore arrangement compensated for the energetic cost of water transfer into and through the hydrophobic pore. As a consequence, water moves into and inside the pore almost as fast as in bulk solution. Although individual permeation events were fast, net fluxes along an osmotic gradient were comparably small. Their calculation required further considerations, for example osmotic pressure in non-equilibrium simulations or even external steering forces [31]. The quantitative values of water permeability, Pf, for simulations from different groups yielded 7.1×10^{-14} [32] and 7.5×10^{-14} cm^3 s^{-1} [30] for the single channel osmotic permeability of mammalian AQP1, which is in excellent agreement with the experimentally determined 5.4×10^{-14} cm^3 s^{-1} [33].

Despite that all molecules move in MD simulations, a stable high-resolution protein structure, that will not collapse, is required for meaningful calculations. Simulations with membrane-embedded mammalian AQP1 at lower resolution (3.8 Å) had identified instabilities of critical residues lining the pore and failed to predict permeation speed correctly [31]. A study investigating the stability of various X-ray structures and homology models revealed that the low resolution structure of mammalian AQP1 did not provide sufficient accuracy for full atomic simulations [34]. Instead, a homology model produced an acceptable description of water inside the channel [34]. The lower resolution open *So*PIP2;1 structure (3.9 Å) also did not have sufficient stability for reliable MD simulations [29]. Homology models of selected aquaporins, that were based on a large number of templates, were more stable during simulations than low(er) resolution structures, such as that of the open *So*PIP2;1 (Dynowski, unpublished). This suggests that simulations should be possible even for those plant aquaporins, for which high-resolution X-ray structures are not yet available.

To reduce calculation times and for a quick routine test of their selectivity, simulations were also performed on monomers. These were compared with those on tetramers, both embedded in lipid bilayers. Both types of simulations gave a similar outcome, indicating that the central tetramer vestibule was of minor importance for the flux of selected solutes [29]. In the computer simulations, usually POPC and/or POPE (1-palmitoyl-2-oleoyl-phosphatidylethanolamine)-lipid membranes without sterols were used, and

direct full conduction events across the lipid membrane were observed for water and other solutes [25, 29, 35, 36]. Such model membranes, however, probably do not adequately reflect the complex properties of a native plant membrane. The artificial simple membranes can be expected to confer lower diffusion barriers for solutes than the native membranes.

Despite their success, the atomic simulations should be treated with caution and their limitations should not be ignored. MD simulations are restricted to rather fast phenomena; this precludes the modeling of relatively slow biological processes and rare events. More recent MD simulations have expanded the simulation times to more than 150 ns, but unusually high solute concentrations or other simplifications were employed to simulate spontaneous permeation events [35]. Furthermore, the lipid/protein complex under study must still be limited to the most important functional units, and starting configurations can bias the system in an undesirable way. Different force field parameters and different computational approaches, such as non-equilibrium and equilibrium simulations, have been used and may have biased the results. Finally, the pH and the transmembrane potential are difficult to implement and are not considered in most studies. Classical MD simulations neglect quantum mechanical effects and therefore do not consider proton diffusion, chemical bond formation, and breakage. On the other hand, the success of MD simulations to quantitatively reproduce experimental parameters, even when different force field parameters were used, strongly validates these computational methods.

H^+ exclusion by aquaporins

In MD simulations, waters were arranged in a bipolar manner inside the pore, meaning that the average dipole orientation reversed in the center of the membrane, close to the NPA region. This arrangement initially suggested that proton transfer might be blocked by a mechanism that disrupts a potential Grotthuss-like proton wire transfer inside the narrow pore [23]. However, this proposal was not confirmed by more sophisticated analysis. Simulations revealed that the large electrostatic barrier impeded H^+ flux [37–40], together with the dehydration cost of moving a proton into the narrow hydrophobic channel [40, 41]. In fact, the large electrostatic barrier excluded protons from permeating even in the presence of an intact proton wire [40, 41].

Voltage clamp measurements on mammalian AQP1 mutants revealed that the arginine of the ar/R filter, which is conserved in most plant aquaporins, had an important impact on proton exclusion [42]. A proton leak was associated with a large pore diameter and the replacement of the arginine from the ar/R filter [42]. The fact that such unconventional mutant pores transported H^+ was convincingly reproduced by MD simulations using sophisticated algorithms [41]. Interestingly, some TIP isoforms, namely TIP1s and *At*TIP5;1, lack the arginine that is critical for proton blockade in AQP1 (Table 1). However, TIP1;1 has been thoroughly investigated with electrophysiology and no H^+-leak was found [43]. There is currently no experimental evidence that any plant aquaporin efficiently transports H^+. The missing arginine in TIP1s may be compensated by neighboring residues and a narrower pore compared to AQP1 mutants. Proton barriers are of exceptional importance in plants, as the acidic apoplast and vesicular/vacuolar lumen are maintained at approximately 2 pH units below that of the cytosol. PIPs, NIPs, and TIPs are thus exposed to a $\sim$100-fold difference in H^+ concentration, which is actively established by the energy consuming proton pumps. We expect that an evolution-driven process efficiently selected for pores that exclude proton transfer across TIPs, while leaving the transport of other substrates intact.

Membrane permeability

The channel-mediated water and solute passage by aquaporins can increase the permeability of a biological membrane by up to two orders of magnitude, depending on the expression level. Since individual aquaporin tetramers within a membrane patch usually occupy only a small fraction of the total membrane area, they will only increase the total membrane permeability when their transport is significantly larger than that of the small lipid membrane area that they occupy.

The intrinsic membrane permeability of a given solute is proportional to its oil–water partition coefficient, its molecular size, and the diffusion coefficient in lipids [1]. For molecules of equal size, the diffusion through the membrane is quicker for those with the greater solubility in lipids. The permeability also depends on the lipid composition and the permeability coefficient for water (P_f) of an artificial lipid bilayer membrane composed of 1-palmitoyl-2-oleoyl phosphatidylcholine (POPC) is $P_f = 7.2 \times 10^{-3}$ cm s^{-1} [2]. Urea diffuses less well across such a membrane ($P_{urea} = 1.3 \times 10^{-6}$ cm s^{-1}), while ammonia permeates more readily, $P_{NH_3} = 3.6 \times 10^{-2}$ cm s^{-1} [2]. The reduction of the membrane fluidity usually reduces the crossing rate of the solute, so that the permeability is often lower in membranes containing 35% POPC, 25% sphingomyelin, and 40% cholesterol: $P_f = 8.5 \times 10^{-3}$ cm s^{-1}, $P_{urea} = 4.4 \times 10^{-8}$ cm s^{-1}, and $P_{NH_3} = 6.8 \times 10^{-3}$ cm s^{-1} [2].

In this context, it is essential to note that biological membranes are more complex. They are composed of

different types of lipids that may form lipid heterogenities, known as lipid rafts, and are packed with integral and associated proteins. Furthermore, plant plasma membranes exhibit a rather high sterol content [44]. The osmotic permeability of native biological membranes is therefore lower than that of artificial membranes. P_f of the yeast plasma membrane was recently measured as $P_f = 2 \times 10^{-4}$ cm s^{-1} [45].

Furthermore, unstirred layers can contribute significantly to, or even dominate, the resistance of a membrane to a given solute. Unstirred layer effects result from the fact that solute concentrations adjacent to the membrane surface differ from the bulk solution, even when the bulk solutions are well mixed [46]. The thickness of unstirred layers is considered to be of particular importance for the volatile CO_2 and artificial lipid bilayers, but does not exceed $\sim$1 µm in small cells [46]. The estimated permeability to CO_2 in 50% POPC and 50% cholesterol was $P_{CO_2} = 3.5 \times 10^{-1}$ cm s^{-1} [47] or tenfold larger [48], but measurements on native membranes have reported values that were more similar to those of NH_3.

Selected plant aquaporins conduct urea

While urea is an important excretion product of nitrogen waste in animals, it is a ubiquitous, rather low-abundant metabolite in plant nitrogen metabolism. Its specific interest for plant physiology stems from its vast agricultural use. Urea (NH_2CONH_2) has become the most popular nitrogen fertilizer by mass in recent years, in part due to its $\sim$15% lower costs compared to other fertilizers. Urea is degraded by soil microorganisms to ammonia and nitrate within days or weeks, but is also directly acquired and utilized by plants [49].

*Nt*AQP1, a PIP1 from tobacco [50], and *Zm*PIP1;5 from maize [51] were reported to conduct at least some urea. However, unlike several mammalian and microbial AQPs that also conducted urea, these PIPs have a narrow, rather water-selective ar/R filter. Other PIPs with the identical ar/R region did not conduct measurable urea, e.g., *At*PIP2;1 [52], and one should be cautious about their relative urea permeability compared to that for water. A low urea permeability has been reported for the plant plasma membrane [53]. Transport measurements with native AQP9 and AQP7, which have a large pore diameter, and mutational analysis in mammalian AQPs, including AQP1 [42], suggested that size selection is an important determinant for urea transport.

In a functional complementation screen using a yeast mutant that lacked the endogenous high affinity urea transport, four TIPs, TIP1;1, TIP1;2, TIP2;1, and TIP4;1, but no NIPs or PIPs, were isolated from a cDNA library from *Arabidopsis* [54]. The TIP transcripts were regulated by the plant nitrogen level and may function in plants to equilibrate urea between the cytoplasm and the vacuole. The fact that the vacuolar membrane is particularly permeable to urea had been identified earlier, and *Nt*-TIPα was suggested to account for this in tobacco [53]. However, the question whether urea transport by TIPs is of physiological relevance has not yet been answered.

A mutational analysis, in which *At*PIP2;1 was exchanged at the ar/R filter into the residues that are found in TIPs and NIPs, indicated that all TIP- and NIP-like pores conducted urea at a sufficiently high rate to promote yeast growth [52]. Urea conduction correlates with the larger pore diameter in TIPs and NIPs [11] and suggested that all native TIPs allow urea passage. Urea transport proved that these mutant aquaporins were functional [52]. The pore requirement for efficient urea transport is explicitly shown for NIP5;1-like mutations in Fig. 1d, e. The urea conductance of the pollen specific *At*TIP5;1 has now been confirmed experimentally [55]. The low urea permeability of PIPs was confirmed by MD simulations on *So*PIP2;1 [52] and other aquaporins [25].

In addition to the ar/R residues, the exchange of residues without direct contact to the pore can indirectly influence the pore diameter [52]. The structural modeling of mutants with altered ar/R filter revealed a threonine in *So*PIP2;1 is crucial to position the phenylalanine side chain of the ar/R. Replacement of the phenylalanine by histidine, as in TIPs (Fig. 1f), required a further concomitant threonine to glycine exchange. Pores were only functional when the histidine was exchanged in combination with the glycine, the residue in TIPs and NIPs (Fig. 1; Table 1).

Although initial studies had proposed that TIP isoforms were localized to different vacuole types, recent studies with GFP-tagged TIP isoforms in *Arabidopsis* have challenged that proposal [56]. All isoforms localized to the same large central vacuole. Vacuolar subdomains may, however, exist as *At*TIP1;1, but not *At*TIP2;1, localized to invaginated bulbs after salt treatment [16]. Although minor differences between the selectivity of TIP isoforms were observed, there is currently little evidence that this property is reflected in physiologically relevant compartment-specific differences.

A PIP-mutant containing the ar/R filter of NIP6;1 transported urea [52], which is in agreement with urea transport by native *At*NIP6;1 in oocytes [11]. However, this urea conductance of *At*NIP6;1 may be of minor physiological importance, as *At*NIP6;1 distributes boric acid in plants, particularly in young and developing shoots [57]. In summary, experimental and computational evidence suggests that size selection is a major determinant for urea conductance in plant aquaporins (Fig. 1e, f), although other factors also contribute to establish efficient urea transport [25, 52].

Permeability of membranes and channels to signaling molecules

Atomic structures provide an estimate on the maximal size of a solute that can enter and pass the pore. However, whether small solutes that pass the size limit are efficiently conducted is difficult to predict from static structures. H_2O_2 has somewhat similar molecular properties as water, can form hydrogen bonds, and has the same permeability as water, $P_{H_2O_2} = 2 \times 10^{-4}$ cm s^{-1}, in yeast [58]. H_2O_2 is a relatively long-lived reactive oxygen species and functions in plants, which are more tolerant to H_2O_2 than animals, as a signaling molecule in abiotic and biotic stresses [59]. The amount of H_2O_2 is dependent on its production, which is compartmentalized to the peroxisomes, mitochondria, chloroplasts, and the apoplast. This is counteracted by complex scavenging redox chemistry in all cellular compartments [60]. The H_2O_2 compartmentation and accumulation had early been visualized with H_2O_2-specific precipitates [61] and other dyes and reactants. H_2O_2 is further produced during the hypersensitive response as a defense reaction to restrict pathogen infection and to confine the pathogen spread outside the plant. Salicylic acid and salt treatment [62] or chilling [18, 63] lead to the extracellular accumulation of reactive oxygen species, including H_2O_2. The same treatments reduced the root water permeability via PIP internalization in *Arabidopsis* roots [62], suggesting that H_2O_2 functions as a common regulator of water homeostasis.

The possibility that aquaporins might conduct hydrogen peroxide had initially been suggested by pressure probe measurements in *Chara*, at huge H_2O_2 concentrations [64]. In a later screen using yeast, AQP8, *Ta*TIP1;1, and *Ta*TIP1;2 were found to conduct H_2O_2, out of 24 candidates [65]. Using a similar experimental setup, further plant aquaporins, including *At*PIP2;1, *At*PIP2;4, and TIP and NIP isoforms, were identified to conduct H_2O_2 [29]. Although the hydrogen peroxide permeability was confirmed with other assays, these studies critically relied on a rather indirect yeast-based growth assay, where H_2O_2 conducting aquaporins caused higher susceptibility to the growth on plates that contained H_2O_2.

Because of the inherent difficulty to experimentally quantify H_2O_2 conduction by PIPs, steered MD simulations were set up with membrane-embedded *So*PIP2;1 (Fig. 2a). A vectorial constant force was applied to the molecules, to increase the probability that the solute entered and crossed the pore within 16 ns. Similar simulations were performed with water. H_2O and H_2O_2 encountered a distinct barrier profile (Fig. 2b) that was estimated from solute trajectories and dwell times in the pore [29]. However, a similar maximal barrier height, close to the ar/R filter, was calculated (Fig. 2). Mutations at the ar/R region, that widened the pore, allowed larger H_2O_2 fluxes [29]. Yeast growth in the presence of H_2O_2 is explicitly shown for mutants that have ar/R filters representative of all PIP, TIP and NIP isoforms of *Arabidopsis* (Fig. 3). Control experiments under non-selective conditions confirmed that these aquaporin mutants did not affect normal growth [29]. Mutants containing ar/R filters of SIPs were not included, since the SIPs are quite divergent in the entire pore and have only very low identity, making homology models less reliable. In accordance with the fact that the ar/R filter was most important for H_2O_2 conduction, these experiments suggest that a larger pore diameter increased the H_2O_2 influx, and triggered cell death (Fig. 3).

In plants, the H_2O_2-induced PIP internalization might also participate in auto-regulating and controlling H_2O_2-signaling. In a chilling-sensitive maize cultivar, chilling increased H_2O_2 levels, which coincided with low water permeability [18]. In contrast, no H_2O_2 accumulation was observed in a tolerant cultivar with high water permeability [18]. These cultivar differences may suggest that the dissipation of high H_2O_2 involved water channels.

Nitric oxide (NO), another signaling molecule, is sufficiently stable to diffuse and communicate between cells. In mammalian cells and liposomes, the rate of NO influx directly correlated with the abundance of AQP1, measured using the NO-specific fluorescent dye diaminofluorescein-2 [66]. Although, intriguingly, earlier studies had suggested that the membrane itself was not a barrier for NO in

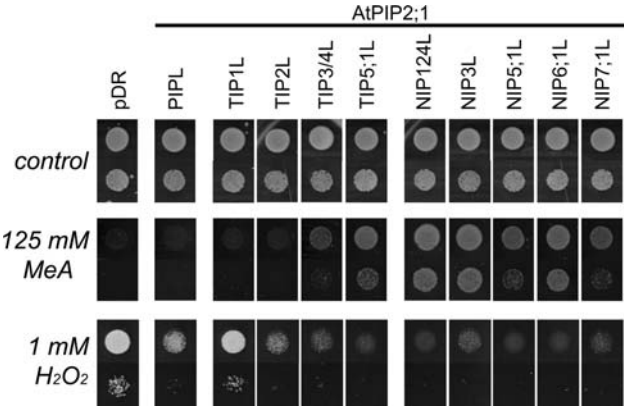

Fig. 3 Mutations in the ar/R region affect the resistance to methylamine and to hydrogen peroxide. *At*PIP2;1 and its pore mutants were expressed in wild type yeast and did not affect growth under non-selective control conditions (*upper panel*). Yeast sensitivity to methylamine (*MeA*, *middle panel*) and H_2O_2 (*lower panel*) was changed by aquaporin mutants. The *lower spot* in each lane corresponds to a 25-fold dilution. All mutants were introduced into *At*PIP2;1 and were expressed from the same plasmid. Mutant nomenclature: NIP1;2-like (NIP1;2L) had ar/R residues as in *At*NIP1;2, etc. The TIP1234L and NIP1234L mutants contained an additional Thr55 to Gly mutation. Yeast survival on MeA correlates with MeA transport capacity (efflux from the cytosol), while survival on H_2O_2 indicates inability to transport H_2O_2

erythrocytes [67]. NO often works in tandem with H_2O_2 and is involved in programmed cell death, pathogen defense, flowering, stomatal closure, and gravitropism in plants [68]. NO evolution and signaling involve different cellular compartments, but whether plant membranes present a barrier for NO diffusion remains unclear. A possible role of PIPs in NO signaling must therefore await a thorough test on aquaporin-deficient mutant plants. Cross-talk with other signaling molecules and the inevitable concomitant loss of water permeability in PIP mutants will complicate the interpretation of possible effects. However, loss-of-function mutants are essential to determine whether the H_2O_2 and/or NO transport through plant aquaporins is of any physiological importance, or just a peculiar side effect without impact.

Molecular requirements for NH_3 conduction and physiological relevance

The first plant aquaporins that conducted ammonia were molecularly identified by yeast complementation. Yeast was transfected with cDNA libraries and only cells expressing TIP2s from wheat and *Arabidopsis* grew under selective conditions [69, 70]. TIP2s have a unique ar/R filter that is distinct from other TIPs, PIPs and NIPs (Table 1). Such library screens usually select for the most abundant cDNAs, while low-abundance channels might have been overlooked with this approach. Indeed, *At*TIP1;2 also complemented the growth defect of a yeast mutant that lacked endogenous ammonium transporters on low ammonia and thus conducted this solute [52]. Correlative evidence suggested that NOD26 channels contribute to the ammonia transfer across peribacteroid membranes [71].

Although yeast growth assays on selective media are easy to perform and straightforward, the growth promotion by aquaporins was much weaker than that by unrelated NH_4^+ transporters [52, 69, 70]. The ammonia transport by human AQP3, AQP7, AQP8, AQP9, and wheat TIP2;1 was measured in oocytes [72]. In that study, NH_3 transport was indirectly deduced via the associated pH change and the secondary induction of ionic currents that result from a large NH_3 influx in oocytes. The large NH_3 permeability of AQP8 was confirmed in lipid bilayer experiments [73], but a loss-of-function mouse did not reveal any physiological function for the ammonia permeability of AQP8 [74]. Whether mammalian AQP1 transports NH_3 is controversial; some studies have suggested that mammalian AQP1 did not conduct NH_3 in yeast and oocytes [42, 69, 72]. In contrast, AQP1 mutants, that had an altered ar/R selectivity filter, transported NH_3 [42]. Other studies using oocytes [75, 76] or red blood cell ghosts [77] identified NH_3 transport by AQP1, but not by AQP5. Since AQP1 and AQP5 have the identical ar/R filter and differ only minimally in their pore [78], their proposed different NH_3 transport activity is quite remarkable [76]. MD simulations on AQP1 revealed that NH_3 encountered a large permeation barrier in the pore and suggested that AQP1 is unlikely to increase NH_3 transport above the intrinsic membrane leak [25].

In AQP8 and TaTIP2;1, ionic currents were associated with ammonia transport when expressed in oocytes. Therefore, these channels were suggested to transport not only NH_3 but in addition H^+, at physiological pH [72]. Whether this H^+ was conducted through the aquaporin pore, or was an "artifact" of the oocyte expression system, remains to be resolved in other expression systems. Oocytes have complex endogenous background currents that are activated by the influx of NH_3. AQP8 excluded H^+ and NH_4^+ in lipid bilayer experiments, at least at low pH [73]. MD simulations revealed that the large electrostatic barrier and the hydrophobic nature of the pore impair the transport of any charged molecule [41]. Since this barrier remains when NH_3 enters the pore, an NH_3-induced H^+ transport appears unlikely.

NH_3 is of similar size as water. The pore diameter thus cannot explain why only some aquaporins conduct NH_3. The mutational exchange of the ar/R filter by two residues in *Ta*TIP2;1 created a channel that excluded NH_3, but had wild type water transport [72]. MD simulations confirmed that the ar/R selectivity filter is the major barrier for NH_3 in plant aquaporins [52]. PIP2;1 pores imposed a large barrier to NH_3, making NH_3 fluxes by PIPs unlikely, in accordance with experimental findings. The barrier for NH_3 did not only result from direct pore-NH_3 interactions themselves, but from perturbations that NH_3 exerted to water–pore interactions at the ar/R filter and to the water arrangement in the pore [52]. This is in agreement with another, more detailed study, where it was similarly concluded that, if the pore diameter is sufficiently large to be passed by the solute, the interactions of water close to the solute in the ar/R region determine whether it is transported at high rate [25]. Since the surrounding water is important for small solute transport, such molecules do not behave as free "gas".

The experimental evidence from native aquaporins and the MD simulations indicated that NH_3 was most efficiently conducted through pores with wide, hydrophobic ar/R filters [25]. This view was challenged by the observation that inhibitor studies had revealed different sensitivities of the water and NH_3 fluxes of TaTIP2;2 expressed in yeast [45]. It was suggested that NH_3 was not transported in the same pore as water, but through a separate pore, possibly the central cavity formed by the tetramer. However, inhibitor studies must be treated with caution, especially when the relatively unspecific Hg^{2+} is

used. Initial inhibitor studies on human AQP3 had suggested different pathways for water and larger solutes, such as urea or glycerol, but this proposal was not substantiated by subsequent studies [79]. Furthermore, the central pore was occluded in the crystal structure of human AQP5 by a lipid, which questions its potential role as solute pathway in some homologs [78].

Although several TIPs allowed NH_3 fluxes, *At*PIP2;1 could not be converted into a NH_3 channel by TIP-like pore mutations. The mutational exchange of the ar/R sites into those resembling TIP1 or TIP2 did not lead to channels that allowed mutant yeast to grow on limiting ammonium [52]. Conversion of a PIP into a NIP-like channel promoted yeast growth on limiting ammonium, suggesting that NIPs conduct NH_3 [52]. The same growth tests were performed on methylamine (MeA, $H_3C–NH_2$, $pK_a = 10.66$) in wild type yeast and are explicitly shown (Fig. 3). MeA is often used as a transport analog of ammonia, but it is possible that methylamine and NH_3 do not share the identical pore requirements for conduction. Yeast-expressing methylamine-conducting channels survived on high MeA, probably due to the passive efflux of the uncharged form of this toxic compound. NIP1, NIP2, NIP3, NIP4, and NIP6-like pores most efficiently rescued growth on NH_3 [52] and MeA (Fig. 3), while TIP3, TIP4, NIP5 and NIP7-like pores were intermediate. No growth complementation was observed for TIP1 and TIP2-like pores, although TIP1s and TIP2s had been experimentally identified as NH_3 channels. It is thus likely that not only the ar/R region, but other parts of the pore are critical for conduction. These residues may be involved in positioning the TIP-like ar/R residues or may recruit NH_3/NH_4^+ to the external entrance. Since the structures of the external pore vestibules of TIPs are not available, a rudimentary NH_4^+ recruitment and de-protonation mechanism, similar to that in ammonium transporters, cannot be excluded in some aquaporins [80]. Finally, the tetrameric pore center may be involved in NH_3 passage.

In accordance with a redundant role for TIPs in the vacuole, over-expression of *At*TIP2;1 [70] or knock-out of the two major TIP1 forms, *At*TIP1;1 and *At*TIP1;2, had little effect on plant growth and metabolism [81]. While there is a general tendency that aquaporins with a wide, hydrophobic ar/R filter conduct at least some NH_3, the exact pore requirements, and whether the central tetramer pore contributes, are still less than clear. Although likely, direct evidence for the physiological relevance of aquaporin-mediated NH_3 fluxes in plants still awaits discovery.

Are plant membranes highly permeable to CO_2 and O_2?

A large number of studies suggested that lipid bilayers and cellular membranes have an exceptionally high permeability to CO_2. This high CO_2 permeability of artificial POPE and POPC membranes was confirmed by MD computer simulations and suggested that these membranes did not provide barriers for CO_2 fluxes [35, 36]. As CO_2 conduction is most frequently indirectly measured, via the associated pH change in the presence of carbonic anhydrase, unstirred layer effects and the diffusion of the associated HCO_3^- are of exceptional importance at physiological pH [47]. In fact, HCO_3^- diffusion, as well as carbonic anhydrase availability in unstirred layers, often limited net CO_2 diffusion across bilayers [47, 48].

Over-expression of mammalian AQP1 in epithelial layers [48], or the double knock-out of AQP1/AQP5 in erythrocytes, did not affect the CO_2 permeability, which argues against their significant CO_2 permeability [82, 83]. Carbonic anhydrase, the enzyme that is used to accelerate the pH changes associated with CO_2 fluxes in some studies, is inhibited by the rather non-specific blocker $HgCl_2$ [82]. This questions the significance of some related experiments that used $HgCl_2$ to block aquaporins. Furthermore, MD simulations showed that the pores of AQP1 and GlpF constitute rather impermeable barriers to CO_2. The central cavity in AQP1 tetramers also imposed a barrier, but this was lower than that of the water pores. Therefore, the central pore was considered as a potential pathway for dissolved CO_2 in unusual membranes with very low intrinsic CO_2 permeability, e.g., when much of the membrane was occupied by integral proteins [25, 35, 36].

Other studies, however, suggest that the intrinsic permeability of membranes can be increased by channels. Specific membranes in the mammalian body were suggested to be rather impermeable to CO_2 [84]. Mass spectrometric determinations of complex CO_2–HCO_3^- equilibrations that involved carbonic anhydrase, suggested that the intrinsic P_{CO_2} was at least one order lower in erythrocytes than the P_{CO_2} predicted by other methods [85]. Erythrocytes lacking AQP1 had less than 50% CO_2 permeability [85]. Reconstituted AQP1 in liposomes also indicated significant CO_2 transport. This study furthermore revealed that CO_2 fluxes were unusual in that they were not affected by changes in membrane fluidity [86]. Research on oocytes expressing carbonic anhydrase had suggested that AQP1 and a pore mutant facilitated CO_2 fluxes, based on cytosolic pH changes measured with impaled pH-electrodes [87]. Using the same method, slightly accelerated pH changes were recorded in oocytes expressing carbonic anhydrase and tobacco *Nt*AQP1. These reflected a 45% increase in CO_2 uptake compared to controls [88]. Considering that several PIPs increased the water permeability of oocytes by more than 20-fold, the 1.45-fold increase in CO_2 transport by *Nt*AQP1 in oocytes was rather small. The H_2O transport, for comparison, was roughly doubled by the expression of *Nt*AQP1 [50]. Additional mammalian

aquaporins were suggested to conduct CO_2 after expression in oocytes [76]. In the latter study, transport was deduced from transient external surface pH changes that were recorded in the absence of carbonic anhydrase. These were not measured from whole cells, but with pH-sensitive electrodes on small membrane patches of $\sim$15 µm diameter.

Direct evidence for a large CO_2 permeability of plant aquaporins is still scarce, but plants with increased PIP expression levels had an improved carbon bio-availability. This was attributed to increased CO_2 transport rates across plant membranes (by *Nt*AQP1) and within leaf tissue [88]. Several other studies confirmed this improved growth by PIP expression and identified that an altered internal CO_2 conductance was affected in PIP mutants. The internal conductance accounts for the movement of CO_2 from the stomatal cavities to the site of carboxylation, which is the enzyme RUBISCO (ribulose 1,5 biphosphate carboxylase) in chloroplasts [89]. RUBISCO has a relatively low affinity for CO_2, and the increased CO_2 bio-availability improves photosynthesis. As a consequence, the CO_2 assimilation rate increased in tobacco leaves that over-expressed *At*PIP1;2 [15] and *Nt*AQP1 [88], and in rice that strongly expressed *Hv*PIP2;1 from barley [90]. PIPs were thus beneficial for plant photosynthesis under favorable conditions, but transgenic tobacco and rice with increased PIP levels were more heavily affected by water stress, due to their higher transpirational water loss [15, 90]. The internal conductance and stomatal opening are considered to be limiting factors for efficient photosynthesis and CO_2 assimilation, and ultimately affect the efficiency of nitrogen and water use in the leaf. The internal conductance increased by 40% in leaves of transgenic rice plants that over-expressed *Hv*PIP2;1, and stomatal aperture and leaf morphology were also changed [90]. In contrast, the internal CO_2 conductance correlated similarly in tobacco with *Nt*AQP1 levels, but other leaf parameters were unchanged [89]. The involvement of aquaporins in determining the internal conductance had already been predicted from experiments with the non-specific inhibitor Hg^{2+} [91].

How the aquaporins increase the internal conductance, a parameter that is experimentally difficult to access, is less clear, but recent work on tobacco sheds light on this issue. *Nt*AQP1 was originally localized to the plasma membrane [22] and vesicular structures [92], but was recently additionally found in the chloroplast envelope [93]. Direct transport measurements on plasma membrane vesicles clarified that the CO_2 permeability of plasma membranes was unchanged by *Nt*AQP1 down-regulation, although the water permeability was about half the magnitude in *Nt*AQP1 RNAi plants [93]. The pH changes associated with the CO_2 transport identified that native chloroplast envelope vesicles had an unusually low permeability to CO_2, approximately fivefold lower than that of the plasma membrane [93]. Genetic reduction of *Nt*AQP1 reduced the CO_2 permeability further, but did not affect the water permeability of these membranes [93]. At the same time, chloroplast envelopes had an about threefold higher water permeability than the plasma membrane, and their water permeability was not affected by *Nt*AQP1. Whether PIP isoforms from other species are also localized and abundant in plastid envelopes should be analyzed in the future, as PIPs have not yet been identified in the plastid proteomes of diverse other plants [94].

Many classical studies suggested that O_2, like CO_2, crosses membranes with an intrinsically high rate, but direct oxygen transport is difficult to measure. MD simulations confirmed the large lipid permeability to oxygen and suggested that mammalian AQP1 and bacterial GlpF impose significant barriers for O_2 fluxes [25, 35]. However, it was considered that in unusual and exceptionally tight membranes, for example with very high protein content, some transport might occur, most likely through the tetramer center.

Although classical experimental evidence and computer simulations collectively exclude that oxygen transport across aquaporins occurs, this has been suggested in animal cells with a high rate of oxygen consumption. AQP1 was induced by low oxygen levels, and hypoxia-inducible gene expression correlated with mammalian AQP1 abundance in a manner that was consistent with O_2 transport by AQP1 [95]. However, direct oxygen transport rates were not measured, and hypoxia-related metabolic by-products might be involved in the AQP1-related regulation.

Interestingly, in *Arabidopsis*, *At*NIP2;1 was transcriptionally up-regulated upon water logging and oxygen deprivation (anoxia) [96]. *At*NIP2;1 only minimally transported water and glycerol, but efficiently transported the uncharged form of lactic acid ($CH_3CH(OH)COOH$), which is synthesized after the metabolic shift from aerobic respiration to lactic acid fermentation in anoxia [96]. The export of lactic acid may contribute to long-term metabolic adaptation to anoxia.

Short-term effects of anoxia include the decrease of water conductance in the root by the rapid closure of PIPs [26]. This mechanism involves cytosolic acidification and PIP gating. Furthermore, a concerted transcriptional down-regulation of PIPs and TIPs upon anoxia leads to a further long-term reduction of water transport in the root [97]. Although there is currently no evidence for O_2 conduction by plant aquaporins, the rapid channel closure upon anoxia would potentially reduce external O_2 supply. It would also restrict further dissipation of the remaining O_2 in the tissue, assuming that these channels hypothetically conduct oxygen.

Specific functions of plant aquaporins in metalloid nutrition and toxicity

It was shown more than a decade ago that some aquaglyceroporins from microorganisms conducted metalloids, potentially as an unspecific side activity [98]. In plants, several NIPs are specifically involved in the regulated uptake and distribution of selected metalloids. Boron is a trace element that is important for proper plant cell wall structure, and in boron-deficient roots, *At*NIP5;1 was upregulated [99]. Its loss reduced the boric acid uptake in roots, lowered biomass production, and increased the sensitivity of roots, shoots, and seeds to boron deficiency [99]. *At*NIP6;1 was also specifically involved in boron homeostasis, despite its capability to transport other solutes [57]. *At*NIP5;1 and *At*NIP6;1 transported boric acid, $B(OH)_3$, when expressed in oocytes [57, 99].

From a mechanistic viewpoint, it is also interesting that these channels transported little (*At*NIP5;1) or no water (*At*NIP6;1), despite their large pore diameter. Similarly, bacterial GlpF had only 17–30% of the water transport capacity of AQP1 [100]. The differential water transport rates in water-selective and less-selective pores with larger diameter has been evaluated using MD simulations, but unexpectedly, the water conductance in GlpF was predicted to exceed that of the narrower water-selective counterpart [101, 102]. The experimentally determined low water conductivity of the wider pores is one of the few details that have not yet been correctly predicted by MD simulations. Residues in the external pore vestibule may be relevant for water exclusion in pores with a wider ar/R filter by electrostatic repulsion. In the aquaglyceroporin of *Plasmodium*, a glutamate in the outer pore vestibule and in proximity to the arginine of the ar/R filter was responsible for high water permeability. A mutation in this glutamate abolished water, but not glycerol transport [103].

Silicic acid, $Si(OH)_4$, which has a slightly larger diameter than boric acid, is a beneficial nutrient for some plants, such as rice, and increases their disease resistance. Silicon accumulates and ultimately irreversibly precipitates on the leaves as amorphous silica or silica gel (SiO_2–nH_2O). The rice mutant lsi1 (low silicon rice 1) was defective in silicon uptake, accumulated less silicon in the shoot, yielded fewer grains, and was more susceptible to disease [104]. This mutant had a defect in the silicon channel *Os*NIP2;1 (Lsi1), which has a unique wide ar/R region (Table 1). This protein showed an in- and efflux capacity for $Si(OH)_4$ when expressed in oocytes and additionally transported urea and boric acid. *Os*NIP2;2 has the same ar/R filter and transported silicic acid in oocytes, while *Os*NIP1;1 and *Os*NIP3;1, which differ in their ar/R region, did not transport silicic acid [105]. A further, very interesting, feature of several NIPs is their polar localization pattern to the outer side of the root cells, allowing vectorial transport of metalloids across epidermal, exodermal, and endodermal lavers [104].

Arsenic is a critical soil contaminant and poses large problems to agriculture in south-east Asia. It exists in different oxidation forms in nature, predominantly as As(V) in aerated soils, but as the reduced form As(III) in paddy soils. While As(V) is a structural analog of phosphate and is transported by phosphate transporters, As(III) mimics $Si(OH)_4$ and is transported by *Os*NIP2;1 (Lsi1) [106]. In paddy rice, arsenite and silicon share the same transport pathway via the roots, which explains why rice is specifically susceptible to arsenic accumulation in contaminated soils. Loss of the silicon influx channel *Os*NIP2;1 (Lsi1) significantly decreased arsenite uptake in rice [106]. Similarly, loss of *At*NIP1;1, which has a different selectivity filter (Table 1), led to *Arabidopsis* that were more resistant to $As(OH)_3$ [107]. Whether the physiological role of *At*NIP1;1 is to facilitate arsenic uptake remains unclear, because most plants may try to exclude arsenic from their cytosol. *At*NIP1;1 is the closest homolog of NOD26 in legumes and has the identical selectivity filter, and correlative evidence suggested that NOD26 conducts water and NH_3. NOD26 is localized in the peribacteroid membrane, which encloses nitrogen-fixing bacteroides in a vesicular compartment [108].

Antimonite, $Sb(OH)_3$, was transported by specific aquaporins in microorganisms and may be transported by NIPs, as there is evidence for channel-like uptake mechanisms in plant roots. Selenium is required in trace amounts for the mammalian diet, but is not essential for plants and may be taken up by NIPs in the form of selenic acid $(HO)_2SeO_2$.

The specificity of NIPs in metalloid transport, together with their already molecularly identified export facilitators, may lead to multiple biotechnological applications. Overexpression of these channels is likely the strategy of choice to overcome low uptake rates in soils, which are deficient in the respective metalloids. Likewise, metalloid excretion, or efflux to the vacuole through modified TIPs, may improve plant growth in areas where contaminant metalloids exceed tolerable levels. Such approaches have already begun for boron [109] and are likely to become of agronomical impact in the near future.

Summary and conclusion

Experimental, structural and computational evidence suggests that plant aquaporins select solutes by two major strategies. Firstly, larger solutes are sterically excluded to permeate narrower pores by size exclusion. Secondly, smaller solutes that can potentially pass the pore diameter

are selected by a hydrophobic mechanism that involves water–protein interactions in the ar/R region. It is likely that the combination of experimental techniques and MD simulations will finally resolve the open questions associated with aquaporin physiology, but despite their value to visualize solute conduction and to predict the selectivity patterns, computer simulations cannot replace experimental work. The detailed analysis of mutant plants will finally resolve the physiological impact of the distinct selectivity of PIPs, TIPs and NIPs. A molecular understanding of aquaporin selectivity and regulation may ultimately help to minimize water losses by cultivated plants, as water shortage gets relevant in increasing areas of the world.

Acknowledgments We thank the Landsgraduiertenförderung Baden-Württemberg and the Deutsche Forschungsgemeinschaft for financial support, and F. de Courcy and R. Kaldenhoff for critically reading the manuscript and discussions.

References

1. Walter A, Gutknecht J (1986) Permeability of small nonelectrolytes through lipid bilayer membranes. J Membr Biol 90:207–217
2. Lande MB, Donovan JM, Zeidel ML (1995) The relationship between membrane fluidity and permeabilities to water, solutes, ammonia, and protons. J Gen Physiol 106:67–84
3. King LS, Kozono D, Agre P (2004) From structure to disease: the evolving tale of aquaporin biology. Nat Rev Mol Cell Biol 5:687–698
4. Maurel C, Verdoucq L, Luu DT, Santoni V (2008) Plant aquaporins: membrane channels with multiple integrated functions. Annu Rev Plant Biol 59:595–624
5. Kaldenhoff R, Fischer M (2006) Functional aquaporin diversity in plants. Biochim Biophys Acta 1758:1134–1141
6. Hachez C, Zelazny E, Chaumont F (2006) Modulating the expression of aquaporin genes in planta: a key to understand their physiological functions? Biochim Biophys Acta 1758:1142–1156
7. Wu B, Beitz E (2007) Aquaporins with selectivity for unconventional permeants. Cell Mol Life Sci 64:2413–2421
8. Bansal A, Sankararamakrishnan R (2007) Homology modeling of major intrinsic proteins in rice, maize and Arabidopsis: comparative analysis of transmembrane helix association and aromatic/arginine selectivity filters. BMC Struct Biol 7:27
9. Tornroth-Horsefield S, Wang Y, Hedfalk K, Johanson U, Karlsson M, Tajkhorshid E, Neutze R, Kjellbom P (2006) Structural mechanism of plant aquaporin gating. Nature 439:688–694
10. Ishikawa F, Suga S, Uemura T, Sato MH, Maeshima M (2005) Novel type aquaporin SIPs are mainly localized to the ER membrane and show cell-specific expression in *Arabidopsis thaliana*. FEBS Lett 579:5814–5820
11. Wallace IS, Roberts DM (2005) Distinct transport selectivity of two structural subclasses of the nodulin-like intrinsic protein family of plant aquaglyceroporin channels. Biochemistry 44:16826–16834
12. Fetter K, Van Wilder V, Moshelion M, Chaumont F (2004) Interactions between plasma membrane aquaporins modulate their water channel activity. Plant Cell 16:215–228
13. Zelazny E, Borst JW, Muylaert M, Batoko H, Hemminga MA, Chaumont F (2007) FRET imaging in living maize cells reveals that plasma membrane aquaporins interact to regulate their subcellular localization. Proc Natl Acad Sci USA 104:12359–12364
14. Martre P, Morillon R, Barrieu F, North GB, Nobel PS, Chrispeels MJ (2002) Plasma membrane aquaporins play a significant role during recovery from water deficit. Plant Physiol 130:2101–2110
15. Aharon R, Shahak Y, Wininger S, Bendov R, Kapulnik Y, Galili G (2003) Overexpression of a plasma membrane aquaporin in transgenic tobacco improves plant vigor under favorable growth conditions but not under drought or salt stress. Plant Cell 15:439–447
16. Boursiac Y, Chen S, Luu DT, Sorieul M, van den Dries N, Maurel C (2005) Early effects of salinity on water transport in Arabidopsis roots. Molecular and cellular features of aquaporin expression. Plant Physiol 139:790–805
17. Alexandersson E, Fraysse L, Sjovall-Larsen S, Gustavsson S, Fellert M, Karlsson M, Johanson U, Kjellbom P (2005) Whole gene family expression and drought stress regulation of aquaporins. Plant Mol Biol 59:469–484
18. Aroca R, Amodeo G, Fernandez-Illescas S, Herman EM, Chaumont F, Chrispeels MJ (2005) The role of aquaporins and membrane damage in chilling and hydrogen peroxide induced changes in the hydraulic conductance of maize roots. Plant Physiol 137:341–353
19. Sakurai J, Ahamed A, Murai M, Maeshima M, Uemura M (2008) Tissue and cell-specific localization of rice aquaporins and their water transport activities. Plant Cell Physiol 49:30–39
20. Forrest LR, Tang CL, Honig B (2006) On the accuracy of homology modeling and sequence alignment methods applied to membrane proteins. Biophys J 91:508–517
21. Wallace IS, Roberts DM (2004) Homology modeling of representative subfamilies of *Arabidopsis* major intrinsic proteins. Classification based on the aromatic/arginine selectivity filter. Plant Physiol 135:1059–1068
22. Biela A, Grote K, Otto B, Hoth S, Hedrich R, Kaldenhoff R (1999) The *Nicotiana tabacum* plasma membrane aquaporin NtAQP1 is mercury-insensitive and permeable for glycerol. Plant J 18:565–570
23. Tajkhorshid E, Nollert P, Jensen MO, Miercke LJ, O'Connell J, Stroud RM, Schulten K (2002) Control of the selectivity of the aquaporin water channel family by global orientational tuning. Science 296:525–530
24. Jensen MO, Park S, Tajkhorshid E, Schulten K (2002) Energetics of glycerol conduction through aquaglyceroporin GlpF. Proc Natl Acad Sci USA 99:6731–6736
25. Hub JS, de Groot BL (2008) Mechanism of selectivity in aquaporins and aquaglyceroporins. Proc Natl Acad Sci USA 105:1198–1203
26. Tournaire-Roux C, Sutka M, Javot H, Gout E, Gerbeau P, Luu DT, Bligny R, Maurel C (2003) Cytosolic pH regulates root water transport during anoxic stress through gating of aquaporins. Nature 425:393–397
27. Verdoucq L, Grondin A, Maurel C (2008) Structure-function analysis of plant aquaporin AtPIP2;1 gating by divalent cations and protons. Biochem J 415:409–416
28. Fischer M, Kaldenhoff R (2008) On the pH regulation of plant aquaporins. J Biol Chem 283:33889–33892
29. Dynowski M, Schaaf G, Loque D, Moran O, Ludewig U (2008) Plant plasma membrane water channels conduct the signaling molecule H_2O_2. Biochem J 414:53–61
30. de Groot BL, Grubmuller H (2001) Water permeation across biological membranes: mechanism and dynamics of aquaporin-1 and GlpF. Science 294:2353–2357
31. Zhu F, Tajkhorshid E, Schulten K (2002) Pressure-induced water transport in membrane channels studied by molecular dynamics. Biophys J 83:154–160

32. Zhu F, Tajkhorshid E, Schulten K (2004) Theory and simulation of water permeation in aquaporin-1. Biophys J 86:50–57
33. Engel A, Stahlberg H (2002) Aquaglyceroporins: channel proteins with a conserved core, multiple functions, and variable surfaces. Int Rev Cytol 215:75–104
34. Law RJ, Sansom MS (2004) Homology modelling and molecular dynamics simulations: comparative studies of human aquaporin-1. Eur Biophys J 33:477–489
35. Wang Y, Cohen J, Boron WF, Schulten K, Tajkhorshid E (2007) Exploring gas permeability of cellular membranes and membrane channels with molecular dynamics. J Struct Biol 157:534–544
36. Hub JS, de Groot BL (2006) Does CO_2 permeate through aquaporin-1? Biophys J 91:842–848
37. de Groot BL, Frigato T, Helms V, Grubmuller H (2003) The mechanism of proton exclusion in the aquaporin-1 water channel. J Mol Biol 333:279–293
38. Chakrabarti N, Tajkhorshid E, Roux B, Pomes R (2004) Molecular basis of proton blockage in aquaporins. Structure 12:65–74
39. Burykin A, Warshel A (2003) What really prevents proton transport through aquaporin? Charge self-energy versus proton wire proposals. Biophys J 85:3696–3706
40. Kato M, Pisliakov AV, Warshel A (2006) The barrier for proton transport in aquaporins as a challenge for electrostatic models: the role of protein relaxation in mutational calculations. Proteins 64:829–844
41. Chen H, Wu Y, Voth GA (2006) Origins of proton transport behavior from selectivity domain mutations of the aquaporin-1 channel. Biophys J 90:L73–L75
42. Beitz E, Wu B, Holm LM, Schultz JE, Zeuthen T (2006) Point mutations in the aromatic/arginine region in aquaporin 1 allow passage of urea, glycerol, ammonia, and protons. Proc Natl Acad Sci USA 103:269–274
43. Maurel C, Reizer J, Schroeder JI, Chrispeels MJ (1993) The vacuolar membrane protein gamma-TIP creates water specific channels in *Xenopus* oocytes. EMBO J 12:2241–2247
44. Uemura M, Joseph RA, Steponkus PL (1995) Cold acclimation of arabidopsis thaliana (effect on plasma membrane lipid composition and freeze-induced lesions). Plant Physiol 109:15–30
45. Bertl A, Kaldenhoff R (2007) Function of a separate NH(3)-pore in aquaporin TIP2;2 from wheat. FEBS Lett 581:5413–5417
46. Barry PH, Diamond JM (1984) Effects of unstirred layers on membrane phenomena. Physiol Rev 64:763–872
47. Gutknecht J, Bisson MA, Tosteson FC (1977) Diffusion of carbon dioxide through lipid bilayer membranes: effects of carbonic anhydrase, bicarbonate, and unstirred layers. J Gen Physiol 69:779–794
48. Missner A, Kugler P, Saparov SM, Sommer K, Mathai JC, Zeidel ML, Pohl P (2008) Carbon dioxide transport through membranes. J Biol Chem 283:25340–25347
49. Merigout P, Lelandais M, Bitton F, Renou JP, Briand X, Meyer C, Daniel-Vedele F (2008) Physiological and transcriptomic aspects of urea uptake and assimilation in *Arabidopsis* plants. Plant Physiol 147:1225–1238
50. Eckert M, Biela A, Siefritz F, Kaldenhoff R (1999) New aspects of plant aquaporin regulation and specificity. J Exp Bot 50:1541–1545
51. Gaspar M, Bousser A, Sissoëff I, Roche O, Hoarau J, Mahé A (2003) Cloning and characterization of ZmPIP1–5b, an aquaporin transporting water and urea. Plant Sci 165:21–31
52. Dynowski M, Mayer M, Moran O, Ludewig U (2008) Molecular determinants of ammonia and urea conductance in plant aquaporin homologs. FEBS Lett 582:2458–2462
53. Gerbeau P, Guclu J, Ripoche P, Maurel C (1999) Aquaporin Nt-TIPa can account for the high permeability of tobacco cell vacuolar membrane to small neutral solutes. Plant J 18:577–587
54. Liu LH, Ludewig U, Gassert B, Frommer WB, Von Wiren N (2003) Urea transport by nitrogen-regulated tonoplast intrinsic proteins in *Arabidopsis*. Plant Physiol 133:1220–1228
55. Soto G, Alleva K, Mazzella MA, Amodeo G, Muschietti JP (2008) AtTIP1;3 and AtTIP5;1, the only highly expressed Arabidopsis pollen-specific aquaporins, transport water and urea. FEBS Lett 582:4077–4082
56. Hunter PR, Craddock CP, Di Benedetto S, Roberts LM, Frigerio L (2007) Fluorescent reporter proteins for the tonoplast and the vacuolar lumen identify a single vacuolar compartment in *Arabidopsis* cells. Plant Physiol 145:1371–1382
57. Tanaka M, Wallace IS, Takano J, Roberts DM, Fujiwara T (2008) NIP6;1 is a boric acid channel for preferential transport of boron to growing shoot tissues in *Arabidopsis*. Plant Cell 20:2860–2875
58. Antunes F, Cadenas E (2000) Estimation of H_2O_2 gradients across biomembranes. FEBS Lett 475:121–126
59. Neill S, Desikan R, Hancock J (2002) Hydrogen peroxide signalling. Curr Opin Plant Biol 5:388–395
60. Foyer CH, Noctor G (2003) Redox sensing and signalling associated with reactive oxygen in chloroplasts, peroxisomes and mitochondria. Physiol Plant 119:355–364
61. Pellinen R, Palva T, Kangasjarvi J (1999) Short communication: subcellular localization of ozone-induced hydrogen peroxide production in birch (*Betula pendula*) leaf cells. Plant J 20:349–356
62. Boursiac Y, Boudet J, Postaire O, Luu DT, Tournaire-Roux C, Maurel C (2008) Stimulus-induced downregulation of root water transport involves reactive oxygen species-activated cell signalling and plasma membrane intrinsic protein internalization. Plant J 56:207–218
63. Lee SH, Singh AP, Chung GC (2004) Rapid accumulation of hydrogen peroxide in cucumber roots due to exposure to low temperature appears to mediate decreases in water transport. J Exp Bot 55:1733–1741
64. Henzler T, Steudle E (2000) Transport and metabolic degradation of hydrogen peroxide in *Chara corallina*: model calculations and measurements with the pressure probe suggest transport of H_2O_2 across water channels. J Exp Bot 51:2053–2066
65. Bienert GP, Moller AL, Kristiansen KA, Schulz A, Moller IM, Schjoerring JK, Jahn TP (2007) Specific aquaporins facilitate the diffusion of hydrogen peroxide across membranes. J Biol Chem 282:1183–1192
66. Herrera M, Hong NJ, Garvin JL (2006) Aquaporin-1 transports NO across cell membranes. Hypertension 48:157–164
67. Liu X, Samouilov A, Lancaster JR Jr, Zweier JL (2002) Nitric oxide uptake by erythrocytes is primarily limited by extracellular diffusion not membrane resistance. J Biol Chem 277:26194–26199
68. Neill S, Bright J, Desikan R, Hancock J, Harrison J, Wilson I (2008) Nitric oxide evolution and perception. J Exp Bot 59:25–35
69. Jahn TP, Moller AL, Zeuthen T, Holm LM, Klaerke DA, Mohsin B, Kuhlbrandt W, Schjoerring JK (2004) Aquaporin homologues in plants and mammals transport ammonia. FEBS Lett 574:31–36
70. Loqué D, Ludewig U, Yuan L, von Wiren N (2005) Tonoplast aquaporins AtTIP2;1 and AtTIP2;3 facilitate NH3 transport into the vacuole. Plant Physiol 137:671–680
71. Niemietz CM, Tyerman SD (2000) Channel-mediated permeation of ammonia gas through the peribacteroid membrane of soybean nodules. FEBS Lett 465:110–114
72. Holm LM, Jahn TP, Moller AL, Schjoerring JK, Ferri D, Klaerke DA, Zeuthen T (2005) NH_3 and NH_4^+ permeability in aquaporin-expressing *Xenopus* oocytes. Pflugers Arch Eur J Physiol 450:415–428

73. Saparov SM, Liu K, Agre P, Pohl P (2007) Fast and selective ammonia transport by aquaporin-8. J Biol Chem 282:5296–5301
74. Yang B, Zhao D, Solenov E, Verkman AS (2006) Evidence from knockout mice against physiologically significant aquaporin 8-facilitated ammonia transport. Am J Physiol Cell Physiol 291:C417–C423
75. Nakhoul NL, Hering-Smith KS, Abdulnour-Nakhoul SM, Hamm LL (2001) Transport of NH(3)/NH in oocytes expressing aquaporin-1. Am J Physiol Renal Physiol 281:F255–F263
76. Musa-Aziz R, Chen LM, Pelletier MF, Boron WF (2009) Relative CO_2/NH_3 selectivities of AQP1, AQP4, AQP5, AmtB, and RhAG. Proc Natl Acad Sci USA 106:5406–5411
77. Ripoche P, Bertrand O, Gane P, Birkenmeier C, Colin Y, Cartron JP (2004) The human rhesus-associated RhAG protein mediates facilitated transport of NH_3 into red blood cells. Proc Natl Acad Sci USA 101:17222–17227
78. Horsefield R, Norden K, Fellert M, Backmark A, Tornroth-Horsefield S, Terwisscha van Scheltinga AC, Kvassman J, Kjellbom P, Johanson U, Neutze R (2008) High-resolution x-ray structure of human aquaporin 5. Proc Natl Acad Sci USA 105:13327–13332
79. Echevarria M, Windhager EE, Frindt G (1996) Selectivity of the renal collecting duct water channel aquaporin-3. J Biol Chem 271:25079–25082
80. Khademi S, O'Connell J 3rd, Remis J, Robles-Colmenares Y, Miercke LJ, Stroud RM (2004) Mechanism of ammonia transport by Amt/MEP/Rh: structure of AmtB at 1.35 Å. Science 305:1587–1594
81. Schussler MD, Alexandersson E, Bienert GP, Kichey T, Laursen KH, Johanson U, Kjellbom P, Schjoerring JK, Jahn TP (2008) The effects of the loss of TIP1;1 and TIP1;2 aquaporins in *Arabidopsis thaliana*. Plant J 56:756–767
82. Yang B, Fukuda N, van Hoek A, Matthay MA, Ma T, Verkman AS (2000) Carbon dioxide permeability of aquaporin-1 measured in erythrocytes and lung of aquaporin-1 null mice and in reconstituted proteoliposomes. J Biol Chem 275:2686–2692
83. Fang X, Yang B, Matthay MA, Verkman AS (2002) Evidence against aquaporin-1-dependent CO_2 permeability in lung and kidney. J Physiol 542:63–69
84. Cooper GJ, Zhou Y, Bouyer P, Grichtchenko II, Boron WF (2002) Transport of volatile solutes through AQP1. J Physiol 542:17–29
85. Endeward V, Musa-Aziz R, Cooper GJ, Chen LM, Pelletier MF, Virkki LV, Supuran CT, King LS, Boron WF, Gros G (2006) Evidence that aquaporin 1 is a major pathway for CO_2 transport across the human erythrocyte membrane. FASEB J 20:1974–1981
86. Prasad GV, Coury LA, Finn F, Zeidel ML (1998) Reconstituted aquaporin 1 water channels transport CO_2 across membranes. J Biol Chem 273:33123–33126
87. Cooper GJ, Boron WF (1998) Effect of PCMBS on CO_2 permeability of *Xenopus* oocytes expressing aquaporin 1 or its C189S mutant. Am J Physiol 275:C1481–C1486
88. Uehlein N, Lovisolo C, Siefritz F, Kaldenhoff R (2003) The tobacco aquaporin NtAQP1 is a membrane CO_2 pore with physiological functions. Nature 425:734–737
89. Flexas J, Ribas-Carbo M, Hanson DT, Bota J, Otto B, Cifre J, McDowell N, Medrano H, Kaldenhoff R (2006) Tobacco aquaporin NtAQP1 is involved in mesophyll conductance to CO_2 in vivo. Plant J 48:427–439
90. Hanba YT, Shibasaka M, Hayashi Y, Hayakawa T, Kasamo K, Terashima I, Katsuhara M (2004) Overexpression of the barley aquaporin HvPIP2;1 increases internal CO(2) conductance and CO(2) assimilation in the leaves of transgenic rice plants. Plant Cell Physiol 45:521–529
91. Terashima I, Ono K (2002) Effects of HgCl(2) on CO(2) dependence of leaf photosynthesis: evidence indicating involvement of aquaporins in CO(2) diffusion across the plasma membrane. Plant Cell Physiol 43:70–78
92. Siefritz F, Biela A, Eckert M, Otto B, Uehlein N, Kaldenhoff R (2001) The tobacco plasma membrane aquaporin NtAQP1. J Exp Bot 52:1937–1953
93. Uehlein N, Otto B, Hanson DT, Fischer M, McDowell N, Kaldenhoff R (2008) Function of *Nicotiana tabacum* aquaporins as chloroplast gas pores challenges the concept of membrane CO_2 permeability. Plant Cell 20:648–657
94. Brautigam A, Hoffmann-Benning S, Weber AP (2008) Comparative proteomics of chloroplast envelopes from C3 and C4 plants reveals specific adaptations of the plastid envelope to C4 photosynthesis and candidate proteins required for maintaining C4 metabolite fluxes. Plant Physiol 148:568–579
95. Echevarria M, Munoz-Cabello AM, Sanchez-Silva R, Toledo-Aral JJ, Lopez-Barneo J (2007) Development of cytosolic hypoxia and HIF stabilization are facilitated by aquaporin 1 expression. J Biol Chem 282:30207–30215
96. Choi WG, Roberts DM (2007) *Arabidopsis* NIP2;1, a major intrinsic protein transporter of lactic acid induced by anoxic stress. J Biol Chem 282:24209–24218
97. Liu F, Vantoai T, Moy LP, Bock G, Linford LD, Quackenbush J (2005) Global transcription profiling reveals comprehensive insights into hypoxic response in *Arabidopsis*. Plant Physiol 137:1115–1129
98. Sanders OI, Rensing C, Kuroda M, Mitra B, Rosen BP (1997) Antimonite is accumulated by the glycerol facilitator GlpF in *Escherichia coli*. J Bacteriol 179:3365–3367
99. Takano J, Wada M, Ludewig U, Schaaf G, von Wiren N, Fujiwara T (2006) The *Arabidopsis* major intrinsic protein NIP5;1 is essential for efficient boron uptake and plant development under boron limitation. Plant Cell 18:1498–1509
100. Saparov SM, Tsunoda SP, Pohl P (2005) Proton exclusion by an aquaglyceroprotein: a voltage clamp study. Biol Cell 97:545–550
101. Hashido M, Ikeguchi M, Kidera A (2005) Comparative simulations of aquaporin family: AQP1, AQPZ, AQP0 and GlpF. FEBS Lett 579:5549–5552
102. Jensen MO, Mouritsen OG (2006) Single-channel water permeabilities of *Escherichia coli* aquaporins AqpZ and GlpF. Biophys J 90:2270–2284
103. Beitz E, Pavlovic-Djuranovic S, Yasui M, Agre P, Schultz JE (2004) Molecular dissection of water and glycerol permeability of the aquaglyceroporin from *Plasmodium falciparum* by mutational analysis. Proc Natl Acad Sci USA 101:1153–1158
104. Ma JF, Tamai K, Yamaji N, Mitani N, Konishi S, Katsuhara M, Ishiguro M, Murata Y, Yano M (2006) A silicon transporter in rice. Nature 440:688–691
105. Mitani N, Yamaji N, Ma JF (2008) Characterization of substrate specificity of a rice silicon transporter, Lsi1. Pflugers Arch 456:679–686
106. Ma JF, Yamaji N, Mitani N, Xu XY, Su YH, McGrath SP, Zhao FJ (2008) Transporters of arsenite in rice and their role in arsenic accumulation in rice grain. Proc Natl Acad Sci USA 105:9931–9935
107. Kamiya T, Tanaka M, Mitani N, Ma JF, Maeshima M, Fujiwara T (2009) NIP1;1, an aquaporin homolog, determines the arsenite sensitivity of *Arabidopsis thaliana*. J Biol Chem 284:2114–2120
108. Wallace IS, Choi WG, Roberts DM (2006) The structure, function and regulation of the nodulin 26-like intrinsic protein family of plant aquaglyceroporins. Biochim Biophys Acta 1758:1165–1175
109. Kato Y, Miwa K, Takano J, Wada M, Fujiwara T (2009) Highly boron deficiency-tolerant plants generated by enhanced expression of NIP5;1, a boric acid channel. Plant Cell Physiol 50:58–66